On the fractal study of LiMn₂O₄ electrode surface

Ali Eftekhari *

Electrochemical Research Center, PO Box 19395-5139, Tehran, Iran

Abstract

Fractal dimension of a LiMn₂O₄ electrode prepared by sol–gel method was determined using electrochemical techniques based on the phenomenon of "diffusion towards electrode surface". A simple discussion was made on the methodology to understand what is really estimated as the fractal dimension. It was demonstrated that the value of fractal dimension determined based on electrochemical methods is strongly dependent on the electrochemical system situation. This is generally true for all real electrodes involving insertion/extraction processes. This comes from the fact that surface morphology of the electrode is subject of significant changes during the electrochemical experiment.
© 2003 Elsevier Ltd. All rights reserved.

Keywords: Fractal dimension; LiMn₂O₄; Surface morphology; Diffusion; Insertion/extraction

1. Introduction

Since 1982 when Le Mehaute et al. [1–3] introduced fractal description to electrochemistry, numerous researchers have attempted to calculate the impedance of the blocking interfaces [4–8]. This attention can be attributed to essential role of electrode surfaces and interfacial problems in electrochemistry. Several methods have been proposed based on different electrochemical techniques for the determination of fractal dimension of electrode surfaces. All of them have been supported by mathematical simulations and experimental evidences. Indeed, electrochemical methods are one of the most useful and reliable methods for the determination of fractal dimension of surfaces. It is very interesting and important, as fractal dimension is a quantitative parameter for analysis of fractal objects, which is widely used for different purposes. In addition, it is one of the most important and useful parameters for analysis of structure of rough surfaces.

Pioneering works of Pajkossy and Nyikos [9–11] to describe time-dependent nature of diffusion towards electrode surfaces generated a new aspect to use various electrochemical techniques for determination of the fractal dimension of electrode surfaces. To gain this efficient approach, a fast electrochemical redox is needed. Oxidation/reduction of the $Fe(CN)_6^{3-}$/ $Fe(CN)_6^{4-}$ redox system at gold surface is sufficiently fast for this purpose, as it has been widely used for such concept. This restricts the determination of fractal dimension, based on electrochemical methods, for artificial gold-coated electrodes. There is a considerable attention to real electrodes in surface electrochemistry and the surface (fractal) analysis of such electrodes for the practical applications is very desirable.

Although, the above-mentioned fast redox cannot be found in the electrochemical redox systems of real electrodes, several researchers have paid a particular attention to this subject [12–17]. The values of fractal dimension of different electrodes determined based on electrochemical methods using their redox systems have been satisfactory, as compared with non-electrochemical methods. However, an important problem, which is not usually taken into account in this context, is the fact that the electrochemical redox systems are usually accompanied by significant surface changes due to the insertion/extraction processes.

As a part of such investigations, the possibility of using Li ion intercalation/deintercalation as a system providing "diffusion towards electrode surface" to determine the fractal dimension of LiMn₂O₄ and similar

---

* Tel.: +98-21-204-2549; fax: +98-21-205-7621.
E-mail address: eftekhari@elchem.org (A. Eftekhari).

compounds has been recently studied [17]. This was of interest due to the importance of such compounds in lithium secondary batteries as the cathode materials. For example, the influence of deposition condition on the fractal dimension of the cathode material deposited has been reported [18]. Interestingly, this approach can also be used for the electrochemical intercalation/deintercalation of Li ions in an aqueous medium [19]. The previous paper [17] was a preliminary one to show this possibility, as typically was examined for a special case. Here, we continue our research to investigate conventional $LiMn_2O_4$ electrodes, which have been widely used for lithium battery performances.

$LiMn_2O_4$ is one of the most promising candidate materials for the preparation of cathodes of lithium secondary batteries due to its valuable advantages, as it is low-cost, non-toxic, abundant, etc. The main disadvantage of $LiMn_2O_4$ is its capacity fades appearing at elevated temperatures, which is mainly due to Mn dissolution. Fortunately, recent developments are in the direction to improve this problem significantly, as simple approaches such as surface modification of the spinel with metal oxides have been proposed to reduce capacity fades of $LiMn_2O_4$ at elevated temperatures [20–25].

In addition, the present research is of interest from methodology point of view, as changes in the surface structure across the electrochemical redox system (at different steps of the intercalation/deintercalation process) are monitored. Although, the results were obtained for the system under investigation, they are applicable for other real electrodes. Indeed, in the context of this paper, it is showed that what is really estimated as the fractal dimension of electrode surfaces based on electrochemical methods.

2. Experimental

The $LiMn_2O_4$ spinel was synthesized according to a known sol–gel method using citric acid as a chelating agent. Manganese acetate was dissolved in water to obtain a saturated solution. Then, lithium acetate was added slowly to this solution while stirring. A saturated aqueous solution of citric acid was added to Li:Mn:citric acid (molar ratio: 1:2:3). The pH of the mixed solution was maintained at 7.0 using addition of ammonium hydroxide solution. The solution was heated at 80 °C for 4 h under a strong stirring condition to remove excess ammonia and water. The precipitated metal citrate was dried in the presence of air at 100 °C for 10 h. The product was decomposed at 300 °C for 6 h in air to eliminate organic contents. Finally, the decomposed powders were slightly ground and then calcined at 600 °C. The heating rate was 1 °C min^{-1}. The detailed analysis of $LiMn_2O_4$ spinel synthesized by this method is found in Ref. [26]. A thin film of $LiMn_2O_4$ with ca. 500 nm thickness was deposited at room temperature using rf power (200 W) under Ar gas pressure of 1.4 Pa using a conventional rf magnetron sputtering.

The electrochemical experiments were carried out in nonaqueous electrolyte solution of 1 M $LiClO_4$ in polyethylene carbonate (PC) using a conventional three-electrode electrochemical cell. The working electrode was a Pt substrate, which was used as current collector for the preparation of $LiMn_2O_4$ cathode. A platinum sheet was used as the counter electrode. All potentials were referenced against Li/Li^+ reference electrode. The electrochemical measurements, at room temperature, were performed using a homemade potentiostat connected to a computer running CORRVIEW software.

The fractal dimension of the $LiMn_2O_4$ electrode was measured using cyclic voltammetry and chronoamperimetry techniques. The corresponding measurements were performed in a conventional nonaqueous medium, which has been widely used for studies of lithium batteries, i.e. $LiClO_4$ in PC. A different approach was also employed for the determination of the fractal dimension of $LiMn_2O_4$ spinel at different states of Li intercalation/deintercalation by gold masking, as different $LiMn_2O_4$ electrodes were prepared by coating their surfaces with a thin uniform layer of gold deposited galvanostatically at a low cathodic current of 10 mA cm^{-2}. Gold masking was performed in a plating bath containing 15 g l^{-1} potassium gold cyanide, 80 g l^{-1} monopotassium phosphate and 70 g l^{-1} potassium citrate. The deposition process was accomplished by passing the required charge for monolayer formation through the cell (more charge was used to assure about the complete gold masking). The thickness of the gold mask was lesser than 2 nm. The fractal analysis of the gold-coated electrodes was carried out using the following experiments.

Electrochemical reaction of ferricyanide on the gold-coated electrode was used as a redox-probe to demonstrate capabilities in the determination of fractal dimension of the $LiMn_2O_4$ electrodes at different states of charge (or discharge). The electrolyte was an aqueous solution of 3 M NaCl and 15 mM $K_4Fe(CN)_6$ and 15 mM $K_3(CN)_6$. The initial potential was 0.6 V versus SCE where no electrochemical reduction of $Fe(CN)_6^{3-}$ occurs. By stepping the potential to low value of 0.0 V, essentially all ferricyanide ions are reduced to $Fe(CN)_6^{4-}$.

Indeed, two different approaches were employed for determination of the fractal dimension of the $LiMn_2O_4$ electrode. Fig. 1 shows the difference of these approaches. Both of them are based on "diffusion towards electrode surfaces", however, the diffusing species are different for two approaches.
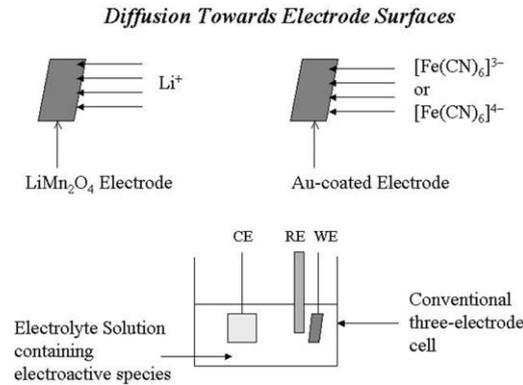
Fig. 1. Schematic of the experimental setup.

3. Results and discussion

Fig. 2 shows a typical cyclic voltammogram of the LiMn$_2$O$_4$ electrode. Six different points (or regions) are distinguished on the cyclic voltammogram corresponding to different states of charge (or discharge). Such points were selected in accordance with the degree of Li intercalation/deintercalation.

It is well known that Li ion intercalation/deintercalation occurs during two steps. The corresponding reactions can be written as (the numbers in the parentheses indicate the state of the reactions shown in Fig. 2):

$$LiMn_2O_4 \ (\mathbf{1}) \rightarrow Li_{0.5}Mn_2O_4 \ (\mathbf{2}) + 0.5Li^+ + 0.5e^- \quad (1)$$
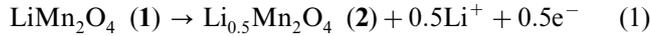
(the reaction accomplished at the first anodic peak)

$$Li_{0.5}Mn_2O_4 \ (\mathbf{2}) \rightarrow Mn_2O_4 \ (\mathbf{3}) + 0.5Li^+ + 0.5e^- \quad (2)$$
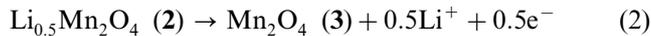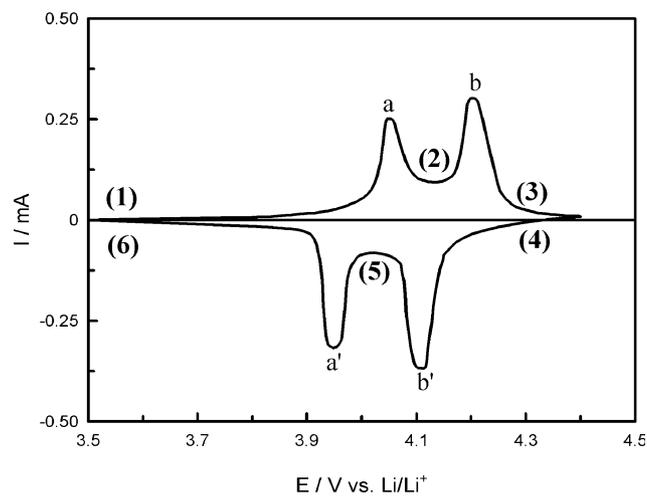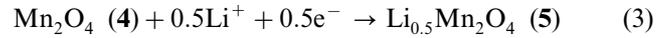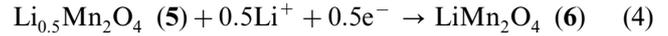
(the reaction accomplished at the second anodic peak)

Fig. 2. Typical cyclic voltammetric characterization of the LiMn$_2$O$_4$ electrode in conventional nonaqueous medium of lithium batteries (1 M LiClO$_4$+PC). The CV shows two redox couples designated as the first (a, a′) and the second (b, b′) pairs of peaks. The points (regions) indicated on the curve correspond to different states of Li$_{1-x}$Mn$_2$O$_4$ spinel formed as the result of progress in the intercalation/deintercalation processes.

$$Mn_2O_4 \ (\mathbf{4}) + 0.5Li^+ + 0.5e^- \rightarrow Li_{0.5}Mn_2O_4 \ (\mathbf{5}) \quad (3)$$

(the reaction accomplished at the second cathodic peak)

$$Li_{0.5}Mn_2O_4 \ (\mathbf{5}) + 0.5Li^+ + 0.5e^- \rightarrow LiMn_2O_4 \ (\mathbf{6}) \quad (4)$$

(the reaction accomplished at the first cathodic peak).

From the chemical formula point of view, $(\mathbf{1}) \equiv (\mathbf{6})$, $(\mathbf{2}) \equiv (\mathbf{5})$ and $(\mathbf{3}) \equiv (\mathbf{4})$. Thus, these four reactions can be re-written as two reversible reactions. Consequently, the Li ion intercalation/deintercalation process of LiMn$_2$O$_4$ is usually expressed in the literature as the following reaction:

$$LiMn_2O_4 = Li_{1-x}Mn_2O_4 + xLi^+ + xe^-$$
$$(0 \leq x \leq 1) \quad (5)$$
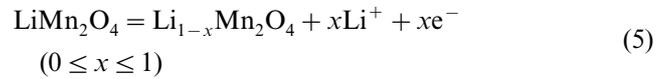
It should be noted that dividing this process to two exactly equal steps $(0 \leq x \leq 0.5$ and $0.5 \leq x \leq 1)$ was made for simplicity of the model proposed. Indeed, choosing x of 0, 0.5 and 1 was for designation of different states. In addition, Mn$_2$O$_4$ was used instead of λ-MnO$_2$ for comparative reason.

Although, this electrochemical redox system (Li$^+$ intercalation/deintercalation into/from LiMn$_2$O$_4$ spinel) is not as fast as the oxidation/reduction occurring for the Fe(CN)$_6^{3-}$/Fe(CN)$_6^{4-}$ redox at gold electrode which is known as the ideal case of "diffusion towards electrode surface", the results reported here are satisfactory for determining the fractal dimension of LiMn$_2$O$_4$ surface based on its associated electrochemical redox.

Similar to the previous work [17], it is possible to use scan rate dependency of the cathodic peak current as described by Stromme et al. [27] to calculate the value of fractal dimension:

$$I_{pc} \propto v^{\alpha} \quad (6)$$

where α is the fractal parameter and can be transformed to the fractal dimension as $\alpha = (D_f - 1)/2$. However, the system under investigation is slightly different from those reported in the literature [12–16]. Usually, the electrochemical redox systems (used for the determination of the fractal dimension) are accompanied by a single reversible couple of peaks, whereas, the electrochemical redox of the system under investigation displays two different redox couples. The problem is that which cathodic peaks should be used to estimate the fractal dimension? In the previous paper [17], we used the second redox couple based on the assumption of stronger electrochemical reaction. Although, that was appropriate for the introducing report, the difference of the fractal dimensions calculated from the scan rate dependencies of two different redox couples should be addressed now.

Fig. 3 illustrates the results obtained from scan rate dependencies of both cathodic peak currents. As seen, there is a significant difference between the fractal dimensions of the LiMn$_2$O$_4$ electrode estimated from
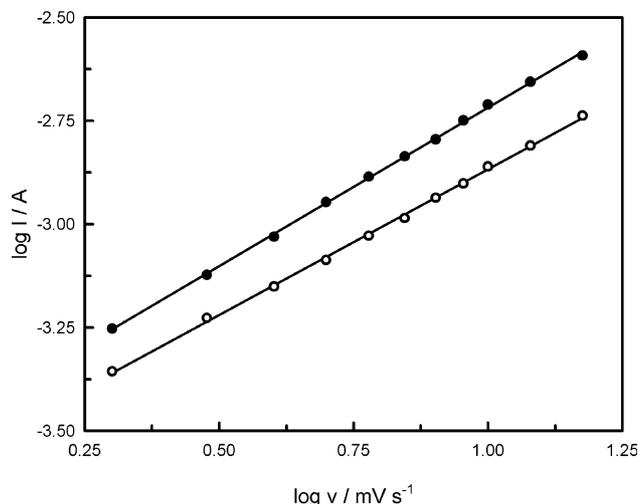
Fig. 3. Scan rate dependencies of the second (●) and the first (○) cathodic peak currents obtained from cyclic voltammograms recorded at different scan rates.

the slopes of the $\log I_{pc}$–$\log v$ plots corresponding to different cathodic peaks. Here, the scan rate dependency of the cathodic peak current was used for determination of the fractal dimension of the $LiMn_2O_4$ electrode surface. This approach is based on the "diffusion towards the electrode surface" phenomenon. The theoretical and mathematical aspects of this method are given in the literature [9–11]. In fact, it is needed to review this phenomenon for the system under investigation. At this stage, there is nothing to do with the anodic voltammogram (forward scan) and the cathodic voltammogram (reverse scan) is just investigated here.

When the system is scanning towards less positive potential during the reverse scan (from 4.4 to 3.5 V vs. Li/Li^+), Reaction (5) is proceeding in the reverse direction. This is needed for the determination of fractal dimension of the electrode surface, i.e. "diffusion towards the electrode surface". The intercalation process is initially started at the beginning of the reverse scan (4.4 V), the $Li_{1-x}Mn_2O_4$ in the reverse direction of Reaction (5) is under the state of $x = 1$ (i.e. Mn_2O_4 (**4**)). Thus, the second cathodic peak indicates the diffusion of Li^+ towards the Mn_2O_4 (**4**) surface. Consequently, scan rate dependency of the second cathodic peak current suggests the fractal dimension of the Mn_2O_4 (**4**) surface. Similarly, it can be concluded that scan rate dependency of the first cathodic peak current suggests the value of the fractal dimension of $Li_{0.5}Mn_2O_4$ (**5**) surface.

Before explaining the difference of the fractal dimensions of these two states of the $LiMn_2O_4$ electrode surface, it is of interest to attempt to determine the fractal dimensions based on chronoamperometry, which has been introduced as a powerful method for fractal analysis of electrode surfaces [28] and even for the system under investigation [17]. Thus, it is needed to use

fully charged state of the $Li_{1-x}Mn_2O_4$ electrode (where $x = 1$) to initiate diffusion of Li^+ towards the electrode surface. By applying the potential of the second cathodic peak at this state of the $LiMn_2O_4$ (Mn_2O_4 (**4**)), Li ions diffuse towards the electrode surface to intercalate into the spinel. During this process, the current decay is proportional to $t^{-\alpha}$ [28]. After this process, it is appropriate to assume that Reaction (3) is fully occurred and the $Li_{1-x}Mn_2O_4$ electrode has achieved the state of $x = 0.5$. Now, chronoamperometric measurements of this partly discharged electrode at the potential of the first cathodic peak can be used to estimate the fractal dimension of the $Li_{0.5}Mn_2O_4$ surface. The chronoamperograms recorded at these two states by applying potentials of the second (Fig. 4a) and first cathodic (Fig. 4c) peaks are presented in Fig. 3 plus the corresponding $\log I_{pc}$–$\log t$ plots (Fig. 4b and d).

As expected the results obtained from both techniques are similar and there is a good agreement between the values estimated for the fractal dimensions of the $LiMn_2O_4$ electrode at two different states (Table 1). Interestingly, it was described that it is possible to determine the fractal dimension of fully charged (not discharged) (Mn_2O_4 (**4**)) or partly charged (partly discharged) ($Li_{0.5}Mn_2O_4$ (**5**)) of the $LiMn_2O_4$ electrode surface. In fact, it is not possible to determine the fractal dimension of own $LiMn_2O_4$ surface based on electrochemical methods, as there is no diffusion process towards $LiMn_2O_4$. This is the limitation of electrochemical methods for the determination of fractal dimensions of real electrode surfaces (based on their redox systems), which is not usually addressed in the literature.

To examine the validity of the results reported and investigation of the fractal structure of the $LiMn_2O_4$ electrode at different regions across the charging/discharging (the points indicated in Fig. 2), it is needed to use a time-independent approach for the determination of the fractal dimension of the $LiMn_2O_4$ electrode at its different states. This means that a physical approach should be employed to avoid any surface changes as a result of the electrochemical reaction during the fractal analysis.

Gold (Au) masking of electrode surfaces is an efficient approach for the determination of their fractal dimensions to capture the fast electrochemical redox of the $Fe(CN)_6^{3-}/Fe(CN)_6^{4-}$ system. Deposition of Au thin-film on metallic surfaces is completely ideal, as provides a uniform surface with the exact structure of the substrate surface [29]. This approach has been successfully used for various cases including artificial fractal electrodes to propose the basic models of diffusion towards electrode surfaces [30]. However, it is not expected such ideal behavior for the case of electrodeposition, as own Au-electrodeposit surface has rough structure [31].
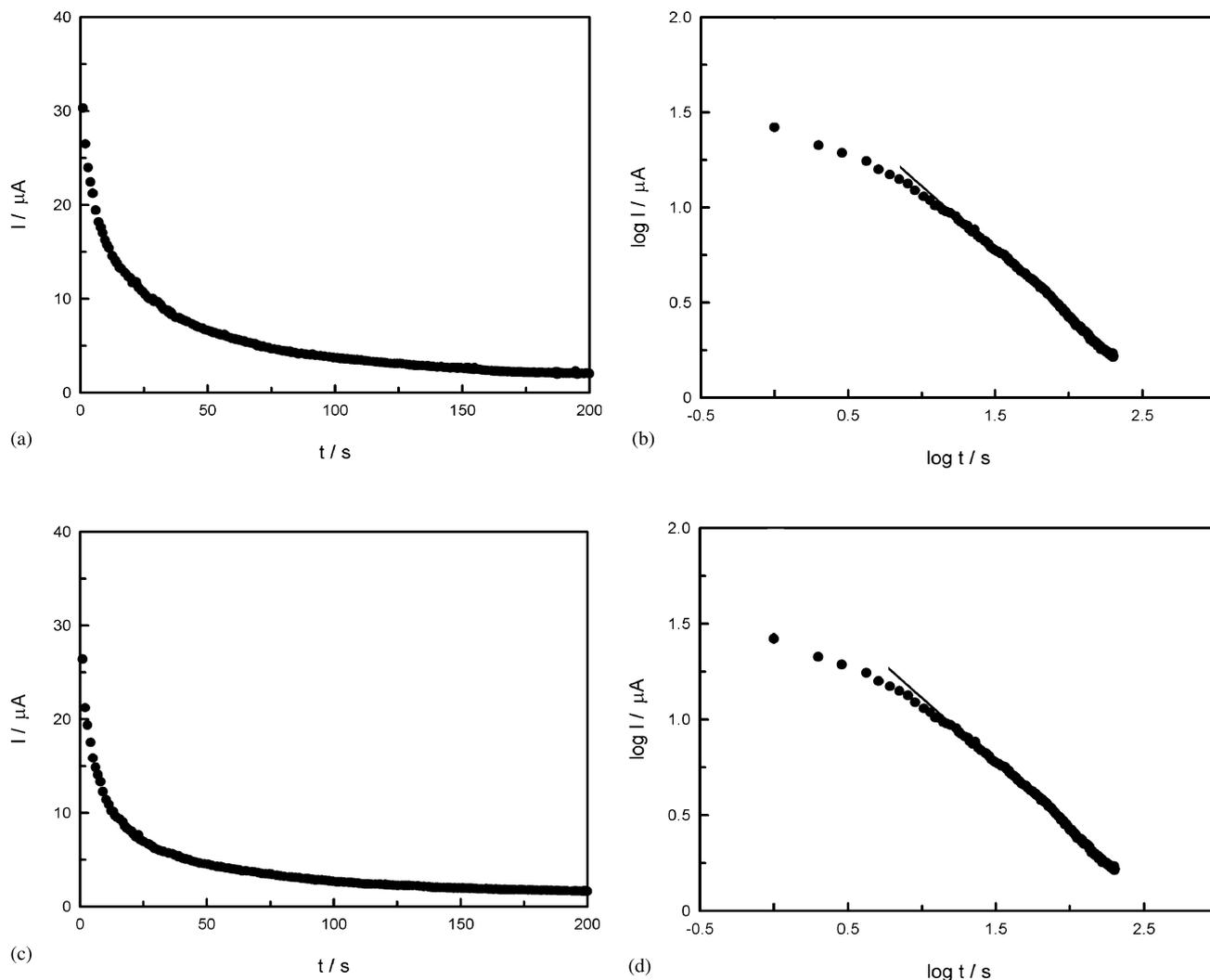
Fig. 4. Chronoamperograms of the $LiMn_2O_4$ electrode (under charged state) recorded at the potentials of the second peak when potential was stepped from 4.0 to 4.01 V (a) and the first peak when potential was stepped from 3.9 to 3.91 V (c). The potentials were estimated from the cathodic peak potentials of the cyclic voltammetric behavior under steady state condition (scan rate approaching zero). (b) and (d) The corresponding $\log I - \log t$ plots.

It is known that electrodeposition of metals is highly dependent on the experimental conditions, e.g. applied potential or current density, plating composition, depositing species concentrations, etc. Thus, it is possible to find an experimental condition for the gold deposition to form a relatively smooth surface. This approach is applicable for different electrode surfaces and the error made due to the roughness of own Au-electrodeposit claim that negligible. There is no claim this approach is able to determine the exact fractal dimension of electrode surfaces, however, the results are satisfactory for the comparative purpose of the present research.

Six different $LiMn_2O_4$ electrodes were prepared at different states of the $LiMn_2O_4$ spinel in accordance with its intercalation/deintercalation process, as indi-

Table 1
Fractal analysis of the $LiMn_2O_4$ electrode at the states (**5**) and (**6**) based on the phenomenon of "diffusion towards electrode surfaces" provided by own redox of the $LiMn_2O_4$ spinel as the result of Li intercalation/deintercalation

Electrode	Cyclic voltammetry			Chronoamperometry		
	α	D_f	R^{2a}	α	D_f	R^{2a}
(**5**)	0.7674	2.535	0.99941	0.7542	2.508	0.98331
(**6**)	0.7042	2.408	0.99900	0.6889	2.378	0.99538

[a] Correlation coefficient.

cated by numbers on the cyclic voltammogram (Fig. 2). The electrode surfaces were covered with a thin film of gold by electrodeposition method. After this action, the $LiMn_2O_4$ electrodes can be considered as gold fractal electrodes and their fractal dimensions were determined based on the well known $Fe(CN)_6^{3-}/Fe(CN)_6^{4-}$ redox system. The results obtained from cyclic voltammetric measurements are presented in Fig. 5.

To achieve an opportunity for comparative study of the results, the data obtained from different experimental measurements are summarized in Table 2. The values determined for the fractal dimension of the $LiMn_2O_4$ electrode at states (4)) and (5) based on gold-masking approach are very close to those obtained previously (Figs. 3 and 4) based on the essential redox of $LiMn_2O_4$ due to Li ion intercalation/deintercalation (the conventional electrochemical methods for the determination of fractal dimension are just available for these two states).

Surprisingly, the values of D_f estimated from the gold-masking approach and the conventional electrochemical methods are approximately the same, whereas, one may expect higher value for the fractal dimension calculated based on the gold-masking approach due to additional roughness of the electrode surface provided by the Au-electrodeposit structure. This failure can be attributed to the fact that due to high roughness of the $LiMn_2O_4$ (with a high fractal dimension), the gold mask cannot cover thoroughly the fractal structure of the electrode surface and some parts with small length scales are missed. Consequently, the fractal dimension of the surface is lesser than that expected. By chance, the additional fractality of the electrode surface provided by
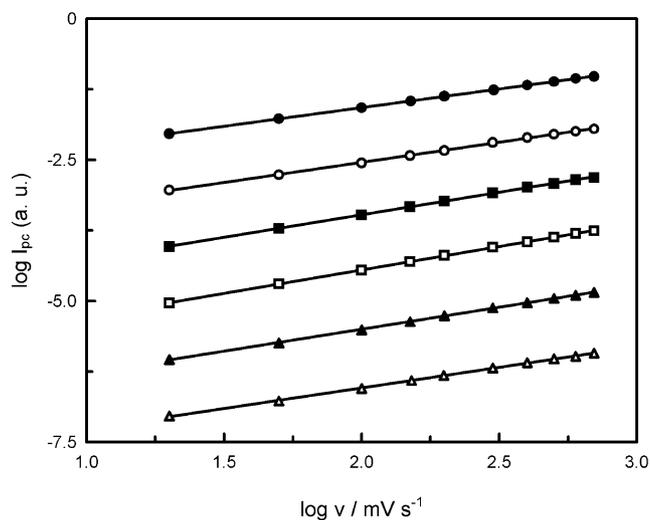
the Au-electrodeposit structure is equal to the fractality of the $LiMn_2O_4$ substrate surface missed in the present case. The fractality of the substrate surface missed is negligible for less complex fractal surfaces (with low fractal dimensions). In addition, one may think that the radius of Au atom is significantly higher than the vacated placed generated as the result of Li ions deintercalation and cannot regularly cover the electrode surface. Although, this is the main failure of this approach and causes the distinction noted above, however, the radius of Au atom is very smaller than the fractality scale (cut-offs) of the $LiMn_2O_4$ [17].

Now, we can assuredly compare the fractal dimensions of six different $LiMn_2O_4$ electrodes obtained from their fractal analysis based on the gold-masking approach. To understand the reason for the appearance of significant changes of the $LiMn_2O_4$ electrode surface during the intercalation/deintercalation process, a simple model of the Li ion intercalation/deintercalation into/from the $LiMn_2O_4$ spinel is presented in Fig. 6. As seen in Fig. 6 and confirmed by the data reported in Table 2, the discharged $LiMn_2O_4$ electrode (1) before the electrochemical intercalation/deintercalation process has the smoother surface. After the first step of the Li extraction (Reaction (1)), the fractal dimension of the electrode surface is increased due to the formation of empty pores provided by the vacated places of Li ions in the $LiMn_2O_4$ spinel (2). This behavior is continued during the second step of the Li extraction (Reaction 2) until the complete Li extraction to form Mn_2O_4 (3), which has the highest value of fractal dimension. The results are obviously indicative of the fact that the fractal dimension of the $LiMn_2O_4$ is increased during the charging process, as Li deintercalation occurs.

As the reverse scan was recorded immediately after the forward scan (charging process), the states designed as (3) and (4) can be considered the same. These two electrodes were taken from the voltammetric behavior at the potential of 4.3 V during the forward and reverse scans, respectively. Thus, the difference of them is just related to 0.2 V potential scan (during forward and reverse scans), and the fractal dimensions estimated by the gold-masking approach are approximately equal (Table 2). However, by comparison of the results obtained from the $LiMn_2O_4$ electrodes (4), (5) and (6) taken during the discharging process (reverse scan of the voltammetric experiment), it can be concluded that the fractal dimension of the $LiMn_2O_4$ electrode decreases during the intercalation process. This can be attributed to the Li^+ intercalation, as fills the vacated places (empty pores) generated on the $LiMn_2O_4$ (as the result of the Li^+ deintercalation). The results showing the changes of surface structure (described by a quantitative factor viz. fractal dimension) are of interest, though, are not different from those expected.

Fig. 5. Scan rate dependencies of the Au-coated $LiMn_2O_4$ electrodes at different states of the intercalation/deintercalation processes of $LiMn_2O_4$ spinel noted in Fig. 2 as (1)–(6). The six $LiMn_2O_4$ electrodes (1) (●), (2) (○), (3) (■), (4) (□), (5) (▲) and (6) (▲-open) obtained from different charging/discharging states (Fig. 2) were coated with a uniform gold mask. Scan rate dependencies of the electrodes were investigated for the fast $Fe(CN)_6^{3-}/Fe(CN)_6^{4-}$ redox at gold surface.

Table 2
Fractal analysis of the $LiMn_2O_4$ electrode at different states (**1**)–(**6**)

Electrode	Fractal parameter α	Fractal dimension D_f	Correlation coefficient R^2
(**1**)	0.6578	2.315	0.99990
(**2**)	0.7117	2.423	0.99946
(**3**)	0.7959	2.592	0.99969
(**4**)	0.8288	2.657	0.99981
(**5**)	0.7768	2.553	0.99969
(**6**)	0.7286	2.457	0.99951

The gold-masking approach was used to gain the process of "diffusion towards electrode surfaces" provided by the fast redox of $Fe(CN)_6^{3-}$/$Fe(CN)_6^{4-}$ system.

In fact, the interesting feature of this study can be perceived by comparison of the electrodes taken during the charging region and those from the discharging. As the fractal dimension of the $LiMn_2O_4$ spinel increased as a result of the deintercalation process, it should be decreased on the same manner during the intercalation process, as the Li ions traveled are returned and the vacated places (empty pores) are filled again. However, the results are significantly different from this expectation. This distinction can be described in accordance with the complicated intercalation process displayed in the Li intercalation/deintercalation model (Fig. 6). Indeed, the Li ions do not exactly fill their original places left during the deintercalation process. Consequently, the surface roughness increases due to irregular intercalation of Li ions. This is more obvious for higher fractal dimensions of the $LiMn_2O_4$ electrode in the states (**5**) and (**6**) in comparison with (**1**) and (**2**).

Another interesting feature, which can be deduced from the comparative study, is related to the difference of the $LiMn_2O_4$ electrode (**1**) and (**6**). Both of them are the same ($Li_{1-x}Mn_2O_4$ where $x = 0$) at the fully discharged state with this difference that (**1**) was as-prepared spinel and (**6**) was obtained after a complete charge/discharge cycle. Similarly, it was found that the fractal dimension of (**3**) or (**4**) is different from the $LiMn_2O_2$ electrode taken from the voltammetric experiment after an additional charging process (another forward scan). This suggests that the fractal dimension of $LiMn_2O_4$ electrode surface (at fully charged or discharged state) is subject of significant changes in the course of cycling, which can be of interest for the practical investigations.

Due to the importance of the changes of $LiMn_2O_4$ surface structure during charging/discharging, a particular attention was paid to investigate the changes the fractal dimension of the $LiMn_2O_4$ in the course of cycling. It is possible by using the approach employed in Fig. 3 and the previous research [17]. Thus, repetitive cyclic voltammetric measurements at different scan rates
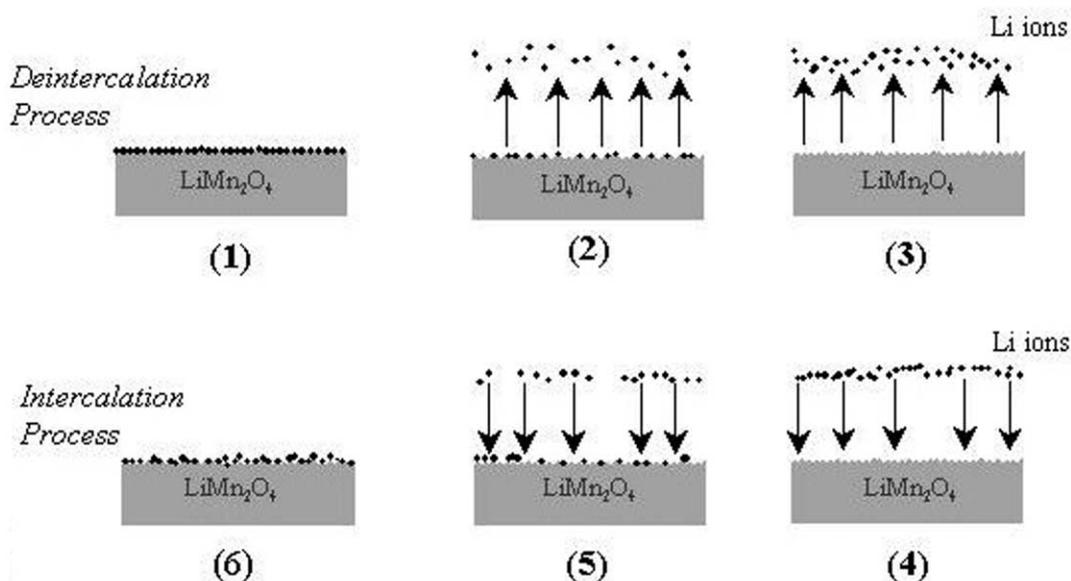

Fig. 6. Simple model of Li ion intercalation/deintercalation into/from $LiMn_2O_4$ spinel during a complete charge/discharge cycle. The black circles indicate Li ions and the white items on the electrode surface denote vacated places (places available for ideal intercalation of Li ions). The numbers noted in bold correspond to different states of the $LiMn_2O_4$ spinel during the intercalation/deintercalation processes as noted in Fig. 2.

were performed. In the latter case, the data collected from cyclic voltammetric measurements of a certain cycle number at different scan rates can be used for the determination of the fractal dimension corresponding to that cycle number. Fig. 7(a) shows such data plotted in a log–log scale to calculated the values of fractal dimension. The changes of the fractal dimension of the $LiMn_2O_4$ electrode as a function of cycle number is illustrated in Fig. 7(b). The curve displayed in Fig. 7(b) shows that the fractal dimension (surface structure) of the $LiMn_2O_4$ electrode is highly dependent on the number of the intercalation/deintercalation processes performed and significant changes occurred during the charge/discharge cycling.

The latter results can be used for the investigation of cycling behavior of $LiMn_2O_4$ cathodes to inspect failure
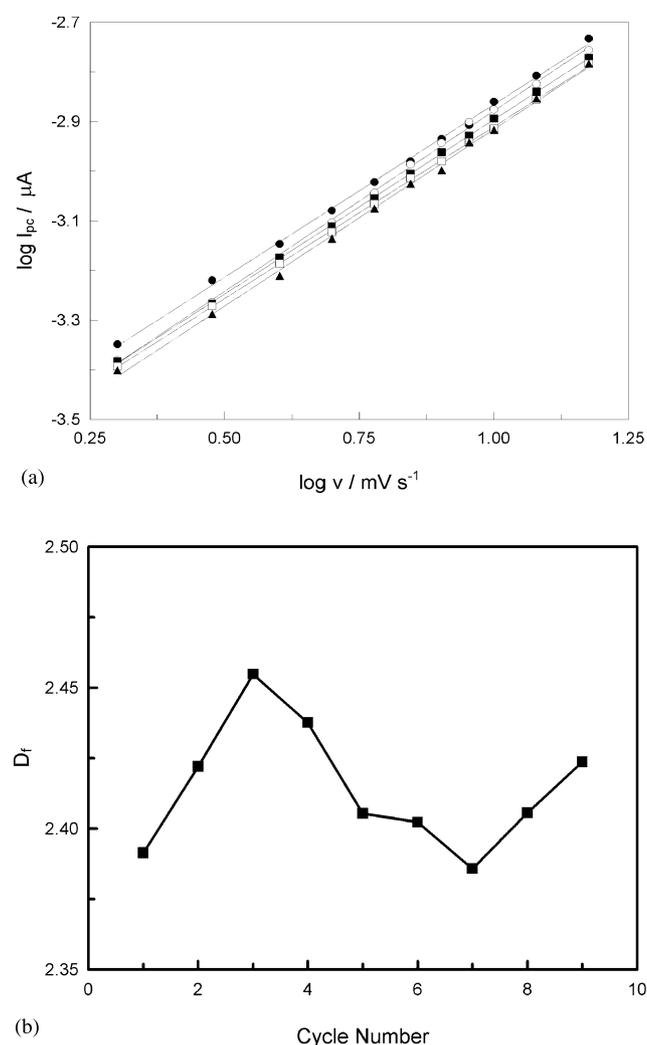

in their cycleability, e.g. capacity fade generated as a result of Mn dissolution, which is highly dependent on the electrode surface structure. However, there is no claim for accurate investigation of this behavior in the system under investigation as a typical case, and this ability is just introduced as an opportunity for the investigation of cathode materials for lithium battery performances. Following our previous paper [17], the present one develops fractal analysis of cathode materials based on electrochemical methods for the achievement of valuable data about their electrochemical behavior.

Although, the discussion made on the fractality of the $LiMn_2O_4$ electrode surface at different states of the intercalation/deintercalation process clarified vague facts of the electrochemical method employed to determine the fractal dimension, an important question propounded at the beginning of the manuscript was remained without answer. What we really measure during fractal analysis of real electrode surfaces based on the phenomenon of "diffusion towards electrode surface"? Let us forget the second peak couple observed in the voltammetric behavior of the $LiMn_2O_4$ electrode (Fig. 2). Like the other redox systems utilized in the literature for the determination of fractal dimension of real electrode surfaces [12–17], the first redox couple (scan rate dependency of the first cathodic peak current) can be used to estimate the values of the fractal dimension of $LiMn_2O_4$ spinel, as "diffusion towards electrode surface" occurs at approximately saturated condition and it can be considered that Li^+ diffusion is under the state that x approaches zero in $Li_{1-x}Mn_2O_4$. This is the main hypothesis to determine the fractal dimension of real electrode surface.

The problem is that intercalation processes are usually incomplete and it is known in battery researches that electrode materials do not reach their theoretical capacity. For the system under investigation, the usual capacity of $LiMn_2O_4$ is about 10–20% lesser than the theoretical capacity of 154 mA h g^{-1}. This is true for most of electroactive materials. Thus, it is inappropriate to address the determination of an electrode surface based on electrochemical methods, while such approaches can just estimate the fractal dimension of only a redox state of the electroactive material. Finally, it can be concluded that comparison of electrochemical methods with non-electrochemical ones for the determination of fractal dimension of electrode surfaces seems to be meaningless, as the first one measures the fractal dimension of partly discharged surface (intercalating ions are still intercalating), whereas, the latter measures the fractal dimension of the original surface (not participated in any intercalation/deintercalation process).

Fig. 7. (a) $\log I_{pc}$–$\log v$ plots obtained from cyclic voltammetric behavior of the $LiMn_2O_4$ electrode in the aqueous electrolyte solution. The data were collected from cyclic voltammograms at different cycle number: 1 (●), 3 (○), 5 (■), 7 (□) and 9 (▲). (b) The values of fractal dimension estimated from the curve slopes plotted against the cycle number.

4. Conclusion

In the context of the present manuscript, the method previously proposed for the determination of fractal dimension of cathode surfaces in lithium battery media was discussed. In addition, another approach was proposed for fractal analysis of the electrode surface at different states of charge and discharge. The latter approach, which is a simple masking method, provides a new opportunity for surface (fractal) analysis of such electrodes based on a simple electrochemical method. A simple description was also made on the determination of fractal dimensions of real electrodes based on their essential redox systems using electrochemical methods to clarify the vague facts (not obviously addressed before) of these methods.

References

[1] A. Le Mehaute, A. de Guibert, M. Delaye, C. Filippi, C.R. Hebd. Seanc. Acad. Sci. 294 (1982) 835.

[2] A. Le Mehaute, G. Crepy, C.R. Hebd. Seanc. Acad. Sci. 294 (1982) 685.

[3] A. Le Mehaute, G. Crepy, Solid State Ionics 9–10 (1983) 17.

[4] S.H. Liu, Phys. Rev. Lett. 55 (1985) 529.

[5] L. Nyikos, T. Pajkossy, Electrochim. Acta 30 (1985) 1533.

[6] T. Kaplan, L.J. Gray, Phys. Rev. B 32 (1985) 7360.

[7] B. Sapoval, Solid State Ionics 23 (1987) 253.

[8] J.C. Wang, Electrochim. Acta 33 (1988) 707.

[9] L. Nyikos, T. Pajkossy, Electrochim. Acta 31 (1986) 1347.

[10] T. Pajkossy, L. Nyikos, Electrochim. Acta 34 (1989) 171.

[11] T. Pajkossy, L. Nyikos, Electrochim. Acta 34 (1989) 181.

[12] W.T. Wu, A.J. McEvoy, M. Gratzel, J. Electroanal. Chem. 291 (1990) 235.

[13] J. Isidorsson, M. Stromme, R. Gahlin, G.A. Niklasson, C.G. Granqvist, Solid State Commun. 99 (1996) 109.

[14] M. Stromme Mattsson, G.A. Niklasson, C.G. Branqvist, Phys. Rev. B 54 (1996) 2968.

[15] K. Malek, Thin Solid Films 408 (2002) 73.

[16] H. Randriamahazaka, V. Noel, C. Chevrot, J. Electroanal. Chem. 521 (2002) 107.

[17] A. Eftekhari, Electrochim. Acta 47 (2002) 4347.

[18] A. Eftekhari, J. Electrochem. Soc., in press.

[19] A. Eftekhari, Electrochim. Acta 47 (2001) 495.

[20] J. Cho, G.B. Kim, H.S. Lim, C.-S. Kim, S.I. Yoo, Electrochem. Solid-State Lett. 2 (1999) 607.

[21] S.S. Kim, Y. Kadoma, H. Ikuta, Y. Uchimoto, M. Wakihara, Electrochem. Solid-State Lett. 4 (2001) A109.

[22] A.M. Kannan, A. Manthiran, Electrochem. Solid-State Lett. 5 (2002) A167.

[23] Y. Shin, A. Manthiram, Electrochem. Solid-State Lett. 5 (2002) A55.

[24] A. Eftekhari, J. Electrochem. Soc. 150 (2003) A966.

[25] A. Eftekhari, J. Power Sources, in press.

[26] B.J. Hwang, R. Santhanam, D.G. Liu, J. Power Sources 97–98 (2001) 443.

[27] M. Stromme, G.A. Niklasson, C.G. Granqvist, Solid State Commun. 96 (1995) 151.

[28] T. Pajkossy, J. Electroanal. Chem. 300 (1991) 1.

[29] C.D. Iocavangelo, K.P. Zarnoch, J. Electrochem. Soc. 138 (1991) 983.

[30] A.R. Imre, L. Balazs, Fractals 8 (2000) 349.

[31] A. Eftekhari, Mendeleev Commun. 12 (2002) 122.